Title

Role of aquaporin water channels in airway fluid transport, humidification, and surface liquid hydration.

Journal

The Journal of general physiology, 117(6)

ISSN

0022-1295

Authors

Song, Y
Jayaraman, S
Yang, B
et al.

Publication Date

2001-06-01

DOI

10.1085/jgp.117.6.573

Peer reviewed

Role of Aquaporin Water Channels in Airway Fluid Transport, Humidification, and Surface Liquid Hydration

Yuanlin Song,*‡ Sujatha Jayaraman,*‡ Baoxue Yang,* Michael A. Matthay,* and A.S. Verkman*‡

From the *Department of Medicine and ‡Department of Physiology, Cardiovascular Research Institute, University of California, San Francisco, California, 94143

ABSTRACT Several aquaporin-type water channels are expressed in mammalian airways and lung: AQP1 in microvascular endothelia, AQP3 in upper airway epithelia, AQP4 in upper and lower airway epithelia, and AQP5 in alveolar epithelia. Novel quantitative methods were developed to compare airway fluid transport–related functions in wild-type mice and knockout mice deficient in these aquaporins. Lower airway humidification, measured from the moisture content of expired air during mechanical ventilation with dry air through a tracheotomy, was 54–56% efficient in wild-type mice, and reduced by only 3–4% in AQP1/AQP5 or AQP3/AQP4 double knockout mice. Upper airway humidification, measured from the moisture gained by dry air passed through the upper airways in mice breathing through a tracheotomy, decreased from 91 to 50% with increasing ventilation from 20 to 220 ml/min, and reduced by 3–5% in AQP3/AQP4 knockout mice. The depth and salt concentration of the airway surface liquid in trachea was measured in vivo using fluorescent probes and confocal and ratio imaging microscopy. Airway surface liquid depth was 45 ± 5 μm and [Na^+] was 115 ± 4 mM in wild-type mice, and not significantly different in AQP3/AQP4 knockout mice. Osmotic water permeability in upper airways, measured by an in vivo instillation/sample method, was reduced by ~40% by AQP3/AQP4 deletion. In doing these measurements, we discovered a novel amiloride-sensitive isosmolar fluid absorption process in upper airways (13% in 5 min) that was not affected by aquaporin deletion. These results establish the fluid transporting properties of mouse airways, and indicate that aquaporins play at most a minor role in airway humidification, ASL hydration, and isosmolar fluid absorption.

KEY WORDS: water permeability • trachea • airway surface liquid • ventilator • fluorescence microscopy

INTRODUCTION

The water-transporting properties of the airways are thought to be important for humidification of inspired air and for maintaining the volume and composition of the airway surface liquid (ASL)[1], the thin fluid layer covering airways. Abnormalities in ASL composition and volume have been proposed to play a major role in the pathophysiology of cystic fibrosis (Quinton, 1994; Noone et al., 1994; Boucher, 1999; Pilewski and Frizzell, 1999; Wine, 1999) and other diseases of the airways such as asthma and bronchitis (Anderson et al., 1982; Yager et al., 1995; Freed and Davis, 1999). Evaporative water loss in the airways is thought to drive water influx from capillaries and interstitium into the ASL by the creation of an osmotic gradient. The depth and ionic composition of the ASL should depend theoretically on the ion transporting properties of the airway epithelium and the rate of evaporative water loss, as well as the water permeability of the airway–capillary barrier. Similarly, the efficiency of airway humidification should depend on the water transporting properties of the airways (Jayaraman et al., 2001a). Measurements of osmotic water permeability by our laboratory (Folkesson et al., 1996; Farinas et al., 1997) and by Matsui et al. (2000) indicate that large and small airways have moderately high osmotic water permeability. However, there is no direct evidence that high water permeability is important in normal airway physiology or in the pathophysiology of cystic fibrosis or other diseases.

Aquaporin water channels are responsible for the high water permeability across many epithelial and endothelial barriers in multiple organ systems. Aquaporins AQP3 and AQP4 are expressed in airway epithelia (Frigeri et al., 1995; King et al., 1997; Nielsen et al., 1997): AQP3 in basal cell plasma membranes in nasopharnyx, trachea, and large bronchi; and AQP4 at the basolateral plasma membrane of columnar surface epithelial cells in small and large airways. AQP1 is expressed throughout the microvascular endothelia in airways and lung (Nielsen et al., 1993, 1997; Hasegawa et al., 1994), and AQP5 is expressed at the luminal membrane of type I alveolar epithelial cells (Nielsen et al., 1997; Funaki et al., 1998). We reported previously

Address correspondence to Alan S. Verkman, M.D., Ph.D., Cardiovascular Research Institute, 1246 Health Sciences East Tower, Box 0521, University of California, San Francisco, San Francisco, CA. 94143-0521. Fax: (415) 665-3847; E-mail: verkman@itsa.ucsf.edu

[1]*Abbreviations used in this paper:* ASL, airway surface liquid; PEEP, positive end expiratory pressure; RT, reverse transcriptase.

that osmotic water permeability across the airspace–capillary barrier in mouse lung is ~10-fold reduced by AQP1 or AQP5 deletion, and >30-fold reduced by AQP1/AQP5 deletion together (Bai et al., 1999; Ma et al., 2000a). AQP4 deletion in AQP1 null mice further reduced water permeability (Song et al., 2000b), implicating a role for AQP4 and the small airways in lung water movement as predicted from earlier microperfusion measurements (Folkesson et al., 1996).

The original purpose of this study was to investigate the role of the four major lung aquaporins in two key airway functions related to fluid transport: airway humidification and regulation of ASL volume and composition. Quantitative in vivo methods were developed to measure humidification in upper and lower airways, ASL volume and salt concentration, and water transport in the upper airways. The hypotheses were tested that aquaporin deletion is associated with defective airway humidification and a hypertonic, dehydrated ASL. In the course of making fluid transport measurements in the upper airways, we discovered amiloride-sensitive isosmolar fluid absorption in upper airways, and so the hypothesis was also tested that aquaporin deletion results in defective fluid absorption by upper airway surface epithelia. Comparative measurements were made in wild-type mice and mice deficient in each of the four lung aquaporins individually and in pairs. The aquaporin knockout mice have been informative in defining the role of aquaporins in peripheral lung physiology (Verkman et al., 2000a) and in extrapulmonary organs (Ma and Verkman, 1999; Verkman et al., 2000b). For example, mice lacking AQP1, AQP2, or AQP3 manifest nephrogenic diabetes insipidus with a severe urinary concentrating defect (Ma et al., 1998, 2000b; Yang et al., 2001a); mice lacking AQP4 have altered cerebral water balance (Manley et al., 2000); and mice lacking AQP5 have defective saliva production (Ma et al., 1999). We find here that although aquaporins facilitate osmotically driven water transport in the airways, they play a minimal role in the physiological important processes of airway humidification, ASL hydration, and isosmolar fluid absorption.

MATERIALS AND METHODS

Transgenic Mice

Transgenic knockout mice deficient in AQP1, AQP3, AQP4, and AQP5 in a CD1 genetic background were generated by targeted gene disruption (Ma et al., 1997, 1998, 1999, 2000b). Measurements were done in litter-matched mice (8–10 wk of age, 20–25 g body weight) produced by intercrossing of heterozygous mice. AQP1/AQP5 and AQP3/AQP4 double knockout mice were generated by serial breeding of single knockout mice to yield double heterozygous mice and then double knockout mice (Ma et al., 2000a; Yang et al., 2001b). The investigators were blinded to genotype information for all measurements. Protocols were approved by the UCSF Committee on Animal Research.

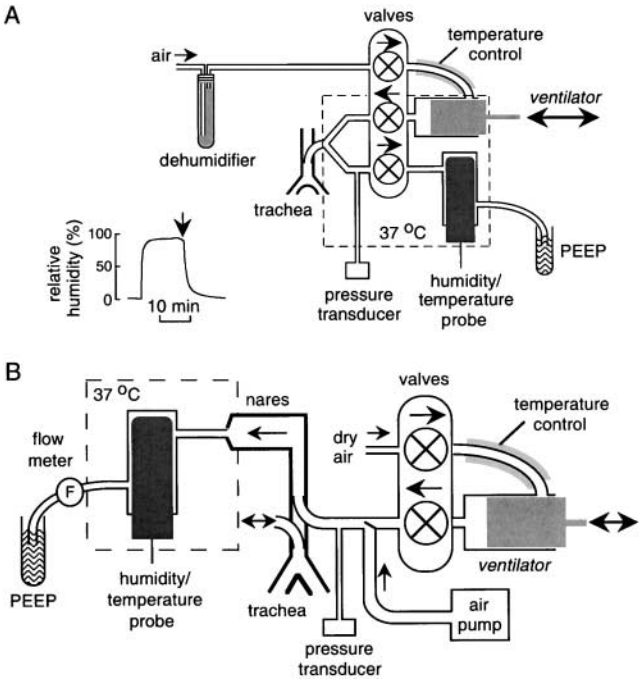

FIGURE 1. Instrumentation for measurement of airway humidification in mice. (A) Measurement of lower airway humidification. After anesthesia, the mouse trachea is cannulated for mechanical ventilation with dry air. Expired air is directed into a chamber containing a humidity sensor. (inset) System efficiency measured using an artificial lung system delivering 100% humidified air. See RESULTS for details. (B) Measurement of upper airway humidification. After anesthesia, a cannula is inserted in the low trachea to permit spontaneous breathing. Dry air from a ventilator or air pump (for rapid constant flow) is passed into a second cannula inserted in the proximal trachea. Air exiting the nares passes into a chamber containing the humidity probe.

Mouse Preparation for Airway Humidification Measurements

Mice were anesthetized with pentobarbital (50 mg/kg, intraperitoneal), and body temperature was maintained at 37 ± 1°C using a heating pad. For lower airway humidification measurements, the midtrachea (0.2–0.3 mm below thyroid gland) was cannulated with a short length (12 mm) of PE-90 tubing attached to a Y-connector. For upper airway humidification measurements, the low trachea (8–9 mm below the thyroid) was cannulated with PE-90 tubing to permit spontaneous breathing. A second tracheotomy was made 3–4 mm proximal to the lower site for inflow of dry air into the upper airways. Gas exiting the upper airways was collected by a tight-fitting plastic mask that covered the nares. The mask was secured with veterinary adhesive (Jorgensen Laboratories, Inc.), and the mouth was separately sealed to force gas exit from the nares. At the completion of the measurements, mice were killed by an overdose of pentobarbital (150 mg/kg, intraperitoneal).

Lower Airway Humidification Measurements

A ventilator circuit was constructed using a constant volume ventilator (model 687; Harvard Apparatus) as shown in Fig. 1 A. Inspired air was dehumidified by passing through a Drierite™ cartridge (Hammond Drierite Co.) or sulfuric acid (no SO_2 gas in inspired air). Inspired air was heated to 37°C by passage through a 40-cm-long stainless steel coil (inner diameter, 1.5 mm) maintained at 37°C. The ventilator output was directed using short non-

compliant tubing into a machined Lucite Y-connector with dead space <0.01 ml. A pressure transducer (model TSD104A; Biopac Systems, Inc.) was used to monitor airway pressure. Expired air passed through the ventilator into a 10-ml Lucite chamber into which was inserted a temperature/relative humidity probe (Cole-Parmer Instrument Co.) having ~15-s response time and better than 1% accuracy in relative humidity determination. Gas exiting the chamber was bubbled under water to set end expiratory pressure. The output arm of the apparatus was maintained at 37°C using an insulated housing into which 37°C dry air was blown. Airway pressure, expired air humidity, and temperature were measured continuously (100 points/s) using an MP100 Biopac workstation.

Upper Airway Humidification Measurements

For measurement of upper airway humidification, the ventilator output or a constant flow of air was directed into the upper tracheostomy (see above) using noncompliant tubing (Fig. 1 B). In most experiments the gas was dry air as described above. The partially humidified air exiting the nares was passed directly into the chamber housing the temperature/humidity probe. Airway pressure was monitored by a pressure transducer, and air flow exiting the Lucite chamber was monitored by an in-line flow sensor (model TRN3300; Kent Scientific Corp.). After ventilation of the upper airways with dry air (8 ml/kg, respiratory rate 100/min) for 10 min, flow was increased to 60, 120, 180, and 220 ml/min using the constant flow pump. Airway pressure, air flow, expired air humidity, and temperature were monitored continuously.

Measurement of ASL Depth and Salt Concentration

Mice were anesthetized with pentobarbital and the trachea was exposed by a midline neck incision. For measurement of ASL depth, a rectangular window (~2 × 3 mm) was cut into the anterior tracheal wall ~3 mm below the thyroid gland (see Fig. 5 A, left). Short transverse incisions were made through adjacent cartilaginous rings. After instillation of fluorescent dye (see below), the tracheal window was sealed using plastic wrap and veterinary tissue adhesive. For measurement of ASL sodium concentration, the fluorescent dye was introduced via a feeding needle, and fluorescence was measured through the translucent tracheal wall. Fluorescence was observed with a Nipkow wheel-type confocal microscope (Leitz, with Technical Instruments K2-Bio coaxial confocal module) using a 50× objective (numerical aperture 0.55, working distance 8.5 mm), appropriate filter sets, and photomultiplier detector. ASL depth was measured by z-scanning confocal microscopy in which fluorescence was recorded continuously during linear translation of the z-focus by 100 μm in <5 s. The ASL was fluorescently stained with tetramethylrhodamine dextran (40,000 D; Molecular Probes) using a dispersion in volatile perfluorocarbon (type FC72, boiling point 56°C; 3M Company) prepared by brief probe sonication. 10 μl of the dispersion was applied onto the ASL using a plastic micropipet. ASL depth was fitted to better than 2 μm accuracy using a reconvolution procedure based on the axial point spread function of the objective as described by Jayaraman et al. (2001b). ASL sodium concentration was determined by ratio imaging using polystyrene beads conjugated with sodium red (Molecular Probes) and Bodipy-fl as described previously (Jayaraman et al., 2001b). In some experiments, a tracheal cannula was inserted above the measurement site and mice breathed dry air (see Fig. 5 B, left).

Osmotic Water Permeability and Isosmolar Fluid Absorption in Upper Airways

Mice were preinjected with atropine (0.2 mg/kg, intraperitoneal), and 5–10 min later anesthetized with pentobarbital (50 mg/kg). After exposure of the trachea by a midline incision, the distal part of trachea (6–8 mm from the thyroid) was cannulated with PE-90 tubing to permit spontaneous respiration. A blunt feeding needle was inserted 5 mm below the thyroid gland through which 50 μl of PBS (325 mOsm containing 1% BSA, for isosmolar fluid absorption) or hyperosmolar saline (325 mOsm plus containing 200 mM sucrose and 1% BSA, for osmotic water permeability) was instilled to fill the upper trachea and nasopharyngeal cavity (see Fig. 6 A). Solutions instilled into the upper trachea/nasopharyngeal cavity contained ^{131}I-albumin (1 μCi/ml) as a volume marker. After specified times, fluid was expelled through the nares by forcing air through the feeding needle and collected in small preweighed vials. Care was taken to avoid evaporative water loss. The vial was weighed and sample ^{131}I radioactivity was measured for computation of ^{131}I-albumin concentration and, hence, fluid dilution or concentration. Mice were killed by pentobarbital overdose after completion of the experiment.

RT-PCR and Immunocytochemistry

Lungs and trachea were harvested from wild-type and aquaporin null mice after euthanasia by pentobarbital overdose. Tissues were immediately homogenized in Trizol reagent (GIBCO BRL) for mRNA isolation using Oligotex mRNA mini kit. After reverse transcription, PCR was carried out using gene-specific primers designed to amplify portions of the coding sequences of each of the nine mouse aquaporins as described previously (Song et al., 2000c). Immunofluorescence localization of aquaporins in 3-4-μm thick cryostat sections of paraformaldehyde-fixed airways and lung was done using purified rabbit polyclonal antibodies as described previously (Frigeri et al., 1995).

RESULTS

Aquaporin Expression in Airways and Lung

Reverse transcriptase (RT)–PCR and immunofluorescence were done to determine the location of aquaporins in mouse airways/lung for design of functional studies. Fig. 2 A shows RT-PCR detection of transcripts encoding mouse aquaporins 1, 3, 4, 5, 7, and 8 in trachea and aquaporins 1, 4, 5, and 8 in peripheral lung. Fig. 2 B shows immunofluorescence of airways (first column) and lung (third column) from wild-type mice with appropriate control tissues from knockout mice lacking each of the aquaporins being stained (second and fourth columns). In airways, AQP1 was expressed in microvascular endothelia, AQP3 in basal airway epithelial cells, and AQP4 was expressed at the basolateral membrane of columnar airway epithelial cells. In airways, AQP1 was expressed in microvascular endothelia, AQP4 at the basolateral membrane of airway epithelial cells, and AQP5 was expressed in alveolar epithelial cells. Staining with anti-AQP7 and AQP8 antibodies was negative (not shown). The results are summarized in Fig. 2 C, and are in agreement with reported data in rat airways and lung. A recent report localized AQP3 to the alveolar epithelium of human lung (Kreda et al., 2001), however, we did not detect AQP3 in peripheral mouse lung by immunofluorescence or RT-PCR. Also, airspace–capillary osmotic water permeability, as mea-

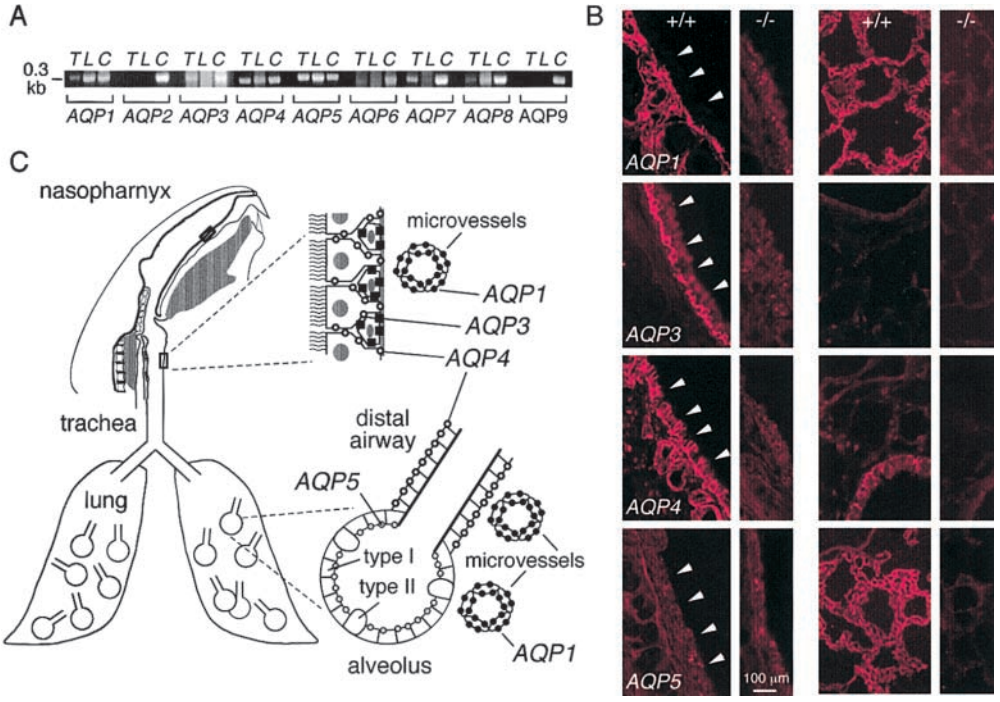

FIGURE 2. Aquaporin water channel expression in mouse airways and lung. (A) RT-PCR analysis of aquaporin transcript expression in trachea (T) and peripheral lung (L). Transcripts corresponding to ~0.3-kb coding sequence fragments of each mouse aquaporin were PCR-amplified using specific primers. Lanes labeled C correspond to amplifications done using a mixture of cDNAs from brain, lung, liver, and kidney, which contained all mouse aquaporins. (B) Immunofluorescence localization of aquaporins 1, 3, 4, and 5 in trachea (wild-type mice, column 1; corresponding knockout mice, column 2) and lung (wild-type mice, column 3, knockout mice, column 4). (arrowheads) Luminal membrane of tracheal epithelium. (C) Schematic of aquaporin expression in airways and lung.

sured by our pleural surface fluorescence method (Carter et al., 1996), was not different in wild-type versus AQP3 null mice (not shown), whereas AQP1 or AQP5 deletion reduced water permeability by ~10-fold (Bai et al., 1999; Ma et al., 2000a).

Humidification in Lower Airways

Lower airway humidification was measured in anesthetized mice that were mechanically ventilated with warm dry air through a tracheotomy as shown in Fig. 1 A. The relative humidity of expired air was monitored continuously by a humidity transducer maintained in a 37°C housing. The system was fitted with air-tight valves, a custom miniature Y-connector, and noncompliant tubing to ensure accurate measurements. The system was tested by verifying relative humidity readings of <2% and >96% when the Y-connector was bypassed and dry or fully humidified air was introduced into the ventilator. In a more stringent test, an artificial lung consisting of a rubber sac

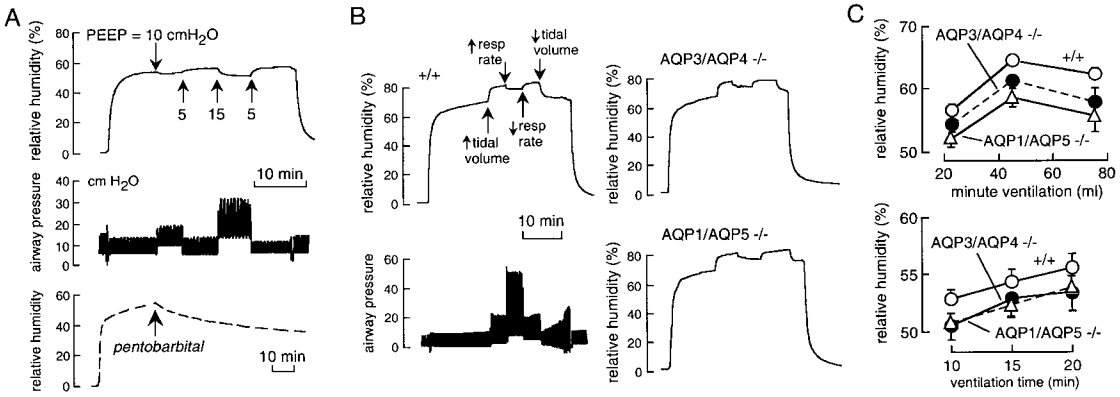

FIGURE 3. Role of aquaporins in lower airway humidification. (A) Time course of expired air humidity (top) and airway pressure (middle) in response to indicated PEEPs. Tidal volume was 8 ml/kg body weight, and the ventilatory rate was 100/min. Bottom curve shows expired air humidity after pentobarbital overdose and cessation of circulation by transection of the abdominal aorta. (B) Representative time courses of expired air humidity in wild-type and double knockout mice of indicated genotype. Also shown (left, bottom) is corresponding airway pressure for wild-type mouse. Initially, mice were ventilated at 100 breaths/min with 8 ml/kg tidal volume. Where indicated, tidal volume was increased to 15 ml/kg and ventilatory rate to 160 per minute. (C) Summary of experiments as done in B (mean ± SEM, n = 4–5 mice) showing expired air humidity at different minute ventilation (top) and at indicated times after ventilation with dry air (bottom).

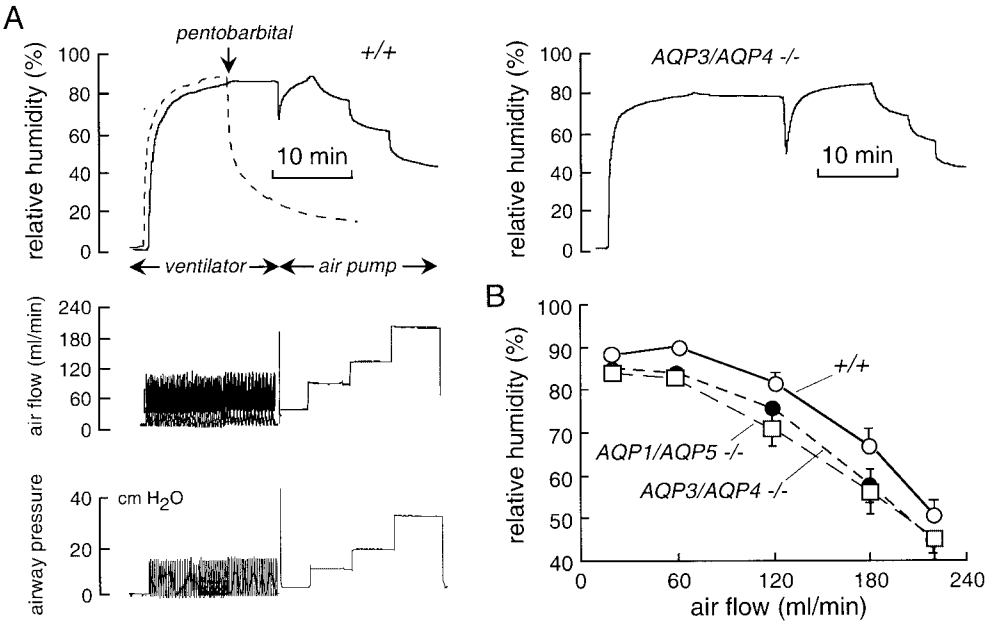

FIGURE 4. Role of aquaporins in upper airway humidification. (A, left) Representative time course of humidity (top), air flow (middle), and airway pressure (bottom) in a wild-type mouse. (right) Same study done on an AQP3/AQP4 double knockout mouse. (B) Averaged relative humidity (mean ± SEM, $n = 5$ mice) in wild-type mice, and AQP3/AQP4 and AQP1/AQP5 double knockout mice as a function of minute ventilation.

with similar compliance to the intact lung was mechanically ventilated with dry air under the same conditions as used in mice. When fully humidified/warmed air was passed into the rubber sac to simulate 100% lung humidification, the recorded relative humidity was in the range of 90–95% (Fig. 1 A, inset), indicating minimal dead space and shunting of dry air through the circuit. Temperature (maintained at 37 ± 0.5°C in the detector circuit) and airway pressure were monitored along with relative humidity in all experiments.

Fig. 3 A shows representative recordings from a wild-type mouse. Initially, a sealed rubber sac was ventilated with dry air, giving a relative humidity of <2% (top). Replacement of the rubber sac by a mouse resulted in increased exhaled air relative humidity to 55–60%. Increased positive end expiratory pressure (PEEP) from 5 to 10 or 15 cm H_2O (Fig. 3 A, middle curve) produced reversible small decreases in relative humidity, probably as a consequence of impaired thoracic venous return. Fig. 3 A (bottom) shows that cessation of circulation (by abdominal aortic transection) during the measurement resulted in a slow decrease in expired air humidity as the lung progressively dehydrated. From the measured initial water loss rate of 0.5 μl/min (computed from relative humidity and minute ventilation) and a mouse lung total water content of ~120 μl (gross weight 150 mg), 10% lung dehydration should occur in ~24 min, in general agreement with the measured time of ~15 min.

Fig. 3 B shows the effects of changing tidal volume and ventilatory rate on exhaled air humidity (left, top) and airway pressure (left bottom; see figure legend for ventilatory parameters). Representative data for double knockout mice lacking the airway water channels AQP3/AQP4 (Fig. 3 B, right, top) and the alveolar water channels AQP1/AQP5 (Fig. 3 B, right, bottom) are shown. Summarized averaged data for a series of wild-type and aquaporin knockout mice indicated a small but significant reduction in lower airway humidification of 2–5% for AQP3/AQP4 deletion, and 4–7% for AQP1/AQP5 deletion (Fig. 3 C).

Humidification in Upper Airways

To measure upper airway humidification, a cannula was inserted in the low trachea to permit spontaneous breathing. Dry air from a ventilator or constant air pump was introduced into the upper airways through a second cannula, and the relative humidity of air exiting the nares was measured (Fig. 1 B). Instrument function was tested by showing identical air flows entering the trachea and exiting the nares, and finding >98% relative humidity when 100% humidified air was introduced into the trachea in place of dry air. Fig. 4 A (left) shows representative curves of relative humidity (top), air flow (middle), and airway pressure (bottom) in a wild-type mouse. Initially, dry air was passed directly into the detection chamber, giving a relative humidity of <2%. Dry air was passed into the trachea from the ventilator, and subsequently, to obtain higher flows, from a constant flow air pump. Upper airway humidification was very efficient (~90%) at physiological minute ventilation, and decreased progressively to <50% at an air flow of 220 ml/min mimicking maximum exercise. The dashed curve in Fig. 4 A (top) shows the rapid decline in humidity after cessation of circulation, as expected from the small total water content of airway tissue compared with lung. A representa-

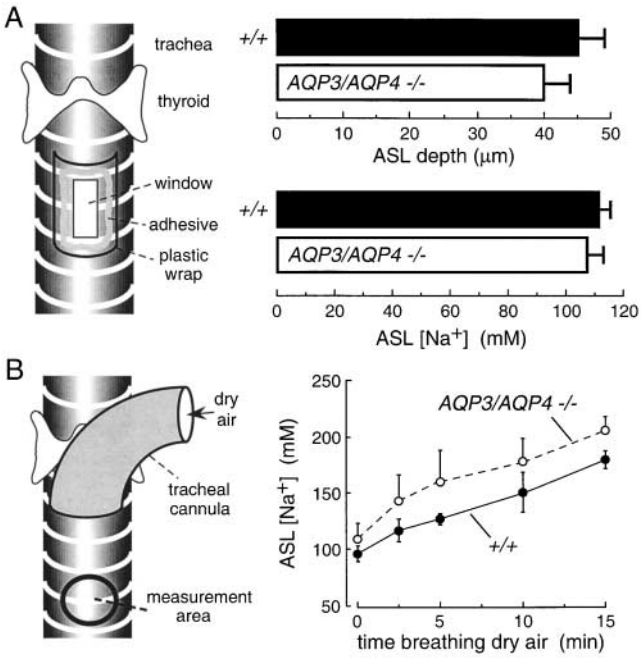

FIGURE 5. Role of aquaporins in hydration of the airway surface liquid (ASL). (A, left) Schematic of approach to measure ASL depth and $[Na^+]$ in anesthetized mice in which a window was created in the trachea for fluorescent dye instillation and z-scanning fluorescence confocal microscopy. (right) ASL depth and $[Na^+]$ in wild-type and AQP3/AQP4 double knockout mice (mean ± SEM, $n = 4$ mice). (B) Measurement of ASL $[Na^+]$ during dry air breathing. (left) Fluorescence was measured through the translucent tracheal wall ("measurement area") below the tip of a tracheal cannula. (right) Time course of ASL $[Na^+]$ in wild-type and AQP3/AQP4 double knockout mice (mean ± SEM, $n = 4$ mice) in response to dry air breathing. Differences in A and B are not significant.

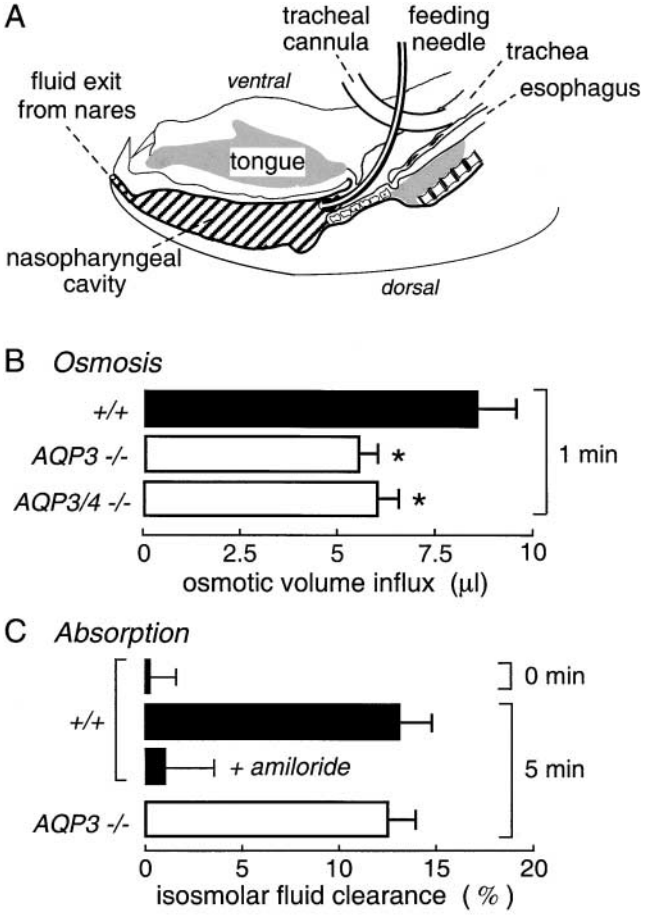

FIGURE 6. Osmotically driven water transport and isosmolar fluid absorption in upper airways. (A) Sagittal section of mouse head showing air spaces in the nasopharnyx and trachea. The trachea was cannulated to permit spontaneous breathing, and isosmolar or hyperosmolar fluid was instilled into the nasopharyngeal cavity by a feeding needle. Fluid was collected into preweighed vials at specified times by passing air through the feeding needle to expel fluid through the nares. The instilled fluid contained ^{131}I-albumin as a volume marker. Data shown as mean ± SEM, with 6–8 mice per condition. See RESULTS for details. (B) Osmotically driven volume influx measured from dilution of the ^{131}I-albumin marker after instillation of 50 μl of a hyperosmolar solution (500 mOsm). (C) Isosmolar fluid absorption (clearance) measured from the increased ^{131}I-albumin concentration at 5 min after instillation of 50 μl of an isosmolar solution (0 min control shown also). Where indicated, 1 mM amiloride was present in the instillate. See RESULTS for explanations. $^*P < 0.01$.

tive experiment for an AQP3/AQP4 double knockout mouse is given in Fig. 4 A (right) and data from a series of wild-type and AQP3/AQP4 and AQP1/AQP5 double knockout mice are summarized in Fig. 4 B. There was a small 3–9% impairment of upper airway humidification in the aquaporin knockout mice.

Hydration of the Airway Surface Liquid

ASL hydration was measured in anesthetized mice in which a transparent window was created in the anterior tracheal wall to permit fluorescent dye introduction and direct visualization of the posterior wall mucosa (Fig. 5 A, left). ASL thickness was measured by z-scanning confocal microscopy, and ASL $[Na^+]$ was measured using a ratiometric $[Na^+]$ indicator as described previously (Jayaraman et al., 2001b). Fig. 5 A (right) shows that neither ASL depth nor $[Na^+]$ were significantly affected by deletion of the airway aquaporins AQP3 and AQP4. To maximally stress the system by increasing evaporative water loss, the tracheal mucosa was exposed to dry air that was breathed spontaneously through a tracheal cannula (Fig. 5 B, left). ASL $[Na^+]$ was measured through the translucent tracheal wall below the cannula. Although ASL $[Na^+]$ increased in response to exposure to dry air as evaporation occurred, there was little effect of AQP3/AQP4 deletion (Fig. 5 B, right).

Upper Airway Osmotic Water Permeability and Isosmolar Fluid Absorption

An in vivo model was developed to determine whether aquaporins facilitate water transport in the upper airways. It was important to maintain normal circulation to

measure osmosis without unstirred layer effects, as well as active fluid transport. Fig. 6 A shows a sagittal section of a mouse head. A cannula was inserted into the distal trachea of an anesthetized mouse to permit spontaneous breathing, and fluid containing ^{131}I-albumin (as a volume marker) was introduced into the nasopharynx via a feeding needle inserted through the wall of the proximal trachea. Fluid volume, assessed from ^{131}I-albumin concentration, was determined at a specified time by forcing air through the feeding needle to expel the nasopharyngeal fluid through the nares.

Initial experiments were done by instilling 50 μl of a physiological solution matched to the mouse serum osmolality of 325 mOsm. Immediate expulsion of fluid after instillation (Fig. 6 C, 0 min) gave no significant change in ^{131}I-albumin concentration, indicating little fluid in the nasopharyngeal cavity under the conditions of the experiments. Osmotically driven water transport across the nasopharyngeal epithelium was measured from the dilution of ^{131}I-albumin at 1 min after instillation of hypertonic fluid (PBS containing 200 mOsm sucrose, 500 mOsm; Fig. 6 B). Prompt ^{131}I-albumin dilution was observed, which was significantly slowed by aquaporin deletion. The absolute osmotic water permeability coefficient (P_f) in wild-type mice was estimated from the osmotic gradient (200 mOsm), the rate of water influx (8.5 μl/min), and estimated nasopharyngeal surface area (~1.8 cm^2) to be ~0.02 cm/s, similar to water permeability of the alveolar–capillary barrier. AQP3 deletion produced an ~35% inhibition of P_f, with no significant further effect of AQP4 deletion. In measurements with instilled isosmolar saline, unexpectedly, the ^{131}I-albumin concentration increased over time, and the increase was inhibited by amiloride (Fig. 6 C), indicating that the nasopharyngeal epithelium can carry out active isosmolar fluid absorption. However, AQP3 deletion, which inhibited osmotically driven water transport, did not affect the rate of active fluid absorption.

DISCUSSION

The goal of this study was to define the role of aquaporin water channels in airway physiology. We studied a set of airway functions that were postulated to require aquaporins, including humidification in upper and lower airways, hydration of the airway surface liquid, and fluid absorption by upper airways. Quantitative measurement of each of these functions in mice required the development and validation of novel methods. We conclude that although aquaporins facilitate osmotically driven water transport in airways, they appear to be of, at most, minor importance in humidification of upper and lower airways, hydration of the airway surface liquid, and isosmolar fluid absorption in upper airways.

The humidification and warming of inspired air has been a subject of long-standing interest. Mammals must adapt to breathing air having widely varying moisture content and temperature, and at rates that can increase more than 10-fold with exercise. Making assumptions about airway geometry, airflow patterns, and blood flow, mathematical models have attempted to predict the efficiency of humidification along the airways (Daviskas et al., 1990; Tsu et al., 1991). Additional complexities are introduced by mouth versus nose versus tracheotomy breathing, and changes in local temperature accompanying evaporation. Although controversy remains, the consensus of the modeling and experimental studies is that the upper airways efficiently warm and humidify air at normal respiratory rates and temperature/moisture content, and that the lower airways complete the humidification process (McFadden, 1992; Williams et al., 1996). However, humidification becomes less efficient during rapid breathing, breathing of dry/cold air, tracheotomy breathing, and in airway disease (Tabka et al., 1988; McFadden, 1992; McRae et al., 1995). Altered airway humidification and ASL hypertonicity have been proposed to play a role in asthma based on the induction of airway reactivity with inhaled hypertonic saline (Willumssen et al., 1994; Freed and Davis, 1999). Motivated by the paucity of data in mice, the conflicting views in the literature, and the complexity of the humidification process, we developed methods to quantify humidification in the upper and lower airways of mice.

Humidification of the lower airways was measured by mechanical ventilation of anesthetized paralyzed mice with dry air. Our instrument accurately measured the relative humidity of expired air to better than 1% accuracy. The lower airways were ~60% efficient at humidifying dry inhaled air. The exact efficiency depended on respiratory rate, tidal volume, and end expiratory pressure, presumably because of differences in airway contact time and secondary changes in venous return and pulmonary blood flow. Humidification efficiencies were quite reproducible from mouse to mouse. Comparison of humidification efficiencies from wild-type and double knockout mice lacking airway water channels (AQP3 and AQP4) or alveolar water channels (AQP1 and AQP5) indicated a small but significant impairment in lower airway humidification. Although the 3–4% impairment in humidification probably has no physiological consequences, the results suggest that both airway and lung aquaporins provide a route for water transport during humidification through a tracheotomy.

Humidification of the upper airways, which is the more relevant parameter for normal nose/mouth breathing, was measured by passing dry air through a tracheostomy and assaying moisture content of air exiting the nares. The mice were allowed to breath spontaneously through a tracheostomy created below the site of dry air entry. As predicted from previous work in

larger animals, we found that the upper airways were highly efficient (>85%) in humidification at physiological ventilatory rates. However, efficiency dropped to <50% when minute ventilation was increased 10-fold to simulate maximum exercise. AQP3/AQP4 or AQP1/AQP5 deletion in double knockout mice reduced the efficiency of upper airway humidification significantly by ~5%. As above, this small effect of aquaporin deletion is probably of little physiological consequence, but it does provide evidence for participation of aquaporins in the humidification process.

The properties of the ASL are thought to be important in the pathophysiology of cystic fibrosis and other diseases of the airways. Two key parameters are the depth and salt concentration of ASL. Our laboratory recently developed noninvasive methods to quantify these parameters in mice using aqueous phase fluorescent indicators that are introduced into the ASL (Jayaraman et al., 2001b). ASL depth was measured by z-scanning confocal microscopy while visualizing the posterior surface of the trachea through a transparent window. ASL depth was 45 ± 5 μm in wild-type mice, not significantly different from 41 ± 3 μm in mice lacking airway water channels AQP3 and AQP4 together. Sodium concentration in the ASL was measured by ratio imaging using a sodium-sensitive fluorescent indicator that was bright, sodium-selective, and sensitive to sodium concentrations in the physiological range. ASL sodium concentration was not significantly different in the double knockout mice. Increasing evaporative water losses by ventilation with dry air resulted in comparable ASL dehydration in wild-type and AQP3/AQP4 double knockout mice. These results provide direct evidence against the hypothesis that aquaporin deletion produces a dehydrated ASL with decreased depth and increased salt concentration. Other factors such as convective fluid transport and intrinsic regulatory processes may be more important than transcellular osmosis in the maintenance of ASL depth and tonicity (Boucher, 1999).

Upper airway water permeability was determined from the dilution of a volume marker in a hyperosmolar instillate introduced into the nasopharynx of living mice. Osmotic water permeability (~0.02 cm/s) was greater than that of trachea and lower airways (0.003–0.006 cm/s) and significantly decreased by AQP3 deletion. An unanticipated finding was that the upper airways in the nasopharynx actively absorb fluid. Isosmolar fluid absorption is well-characterized in peripheral lung (Matthay et al., 1996), but to our knowledge has not been reported in nasopharynx. Physiologically, isosmolar fluid absorption may protect the upper airways from fluid overload resulting from upward ciliary convection of fluid, gland secretions, and aspiration. The rapid fluid absorption may also protect the glottis and maintain upper airway patency during ventilation. As found for isosmolar fluid absorption in peripheral lung (Bai et al., 1999; Ma et al., 2000a), aquaporin deletion did not affect fluid absorption in the nasopharynx. The substantially slower rates of active fluid transport in nasopharnyx and alveolus compared with proximal tubule (Schnermann et al., 1998) and salivary gland (Ma et al., 1999) probably account for the lack of effect of aquaporin deletion.

We previously examined the roles of AQP1, AQP4, and AQP5 in peripheral lung physiology, where the proposed aquaporin functions included alveolar fluid clearance, gas exchange, and adaptation to acute and subacute lung injury. The principal finding was that although these aquaporins provide a major route for osmotically driven water transport among the airspace, interstitial, and capillary compartments, they are not required for physiologically important lung functions (Verkman et al., 2000a). Whereas osmotic water permeability was >30-fold reduced by deletion of AQP1 and AQP5, active near isosmolar alveolar fluid clearance was not affected (Ma et al., 2000a). The rapid reabsorption of fluid from the airspace just after birth was not impaired by aquaporin deletion (Song et al., 2000a). Further, aquaporin deletion did not affect the response of the adult lung in models of lung injury, including acid-induced epithelial injury, thiourea-induced endothelial injury, and hyperoxic subacute lung injury (Song et al., 2000a). Lung carbon dioxide transport, which was proposed from oocyte expression studies to be facilitated by AQP1 (Nakhoul et al., 1998), was not impaired in AQP1 null mice (Yang et al., 2000). Recently, the role of aquaporins in pleural fluid physiology was examined (Song et al., 2000c). Deletion of the principal aquaporin in pleural microvasculature and surface cells (AQP1) resulted in a substantially decreased osmotic water permeability of the pleural surface. However, physiologically important pleural functions, including the formation and resolution of pleural effusions, were not affected by AQP1 deletion. Thus, in peripheral lung and pleura, the aquaporins do not appear to be physiologically important despite their major role in airspace–capillary osmosis.

The airway studies reported here addressed a series of different physiological functions that are predicted to require aquaporins: upper and lower airway humidification, airway surface liquid hydration, and isosmolar fluid absorption in upper airways. We conclude that aquaporins are of minor importance in these processes. As discussed previously (Verkman et al., 2000b), the tissue-specific expression of an aquaporin does not ensure physiological significance. As in peripheral lung and pleura, the relatively low rates of fluid movement in the airways, even under maximal stress, are substantially lower than those in kidney, salivary gland, and other tissues where aquaporins are required for normal function. It remains unclear why aquaporins are expressed in numerous loca-

tions without a demonstrable physiological function. The results here provide direct evidence against a role of aquaporins in airway fluid transport physiology under normal physiological conditions and in response to selected stresses such as rapid ventilation with dry air. However, the possibility cannot be excluded that airway aquaporins might facilitate airway fluid transport in response to stresses not tested here or serve alternative functions to be discovered.

We thank Ms. Liman Qian for transgenic mouse breeding and genotype analysis. This study was supported by the National Institute of Health grants HL59198, HL51854, DK35124, HL60288, and DK43840, and grant R613 from the National Cystic Fibrosis Foundation.

Submitted: 27 March 2001
Revised: 2 May 2001
Accepted: 3 May 2001

REFERENCES

Anderson, S.D., R.E. Schoeffel, R. Follet, C.P. Perry, E. Daviskas, and M. Kendall. 1982. Sensitivity to heat and water loss at rest and during exercise in asthma patients. *Eur. J. Respir. Dis.* 63:459–471.

Bai, C., N. Fukuda, Y. Song, T. Ma, M.A. Matthay, and A.S. Verkman. 1999. Lung fluid transport in aquaporin-1 and aquaporin-4 knockout mice. *J. Clin. Invest.* 103:555–561.

Boucher, R.C. 1999. Molecular insights into the physiology of the 'thin film' of airway surface liquid. *J. Physiol.* 516:631–638.

Carter, E.P., M.A. Matthay, J. Farinas, and A.S. Verkman. 1996. Transalveolar osmotic and diffusional water permeability in intact mouse lung measured by a novel surface fluorescence method. *J. Gen. Physiol.* 108:133–142.

Daviskas, E., I. Gonda, and S.D. Anderson. 1990. Mathematical modeling of heat and water transport in human respiratory tract. *J. Appl. Physiol.* 69:362–372.

Farinas, J., M. Kneen, M. Morre, and A.S. Verkman. 1997. Plasma membrane water permeability of cultured cells and epithelia measured by light microscopy spatial filtering. *J. Gen. Physiol.* 110: 283–296.

Folkesson, H., M.A. Matthay, A. Frigeri, and A.S. Verkman. 1996. High transepithelial water permeability in microperfused distal airways: evidence for channel-mediated water transport. *J. Clin. Invest.* 97:664–671.

Freed, A.N., and M.S. Davis. 1999. Hyperventilation with dry air increase airway surface fluid osmolality in canine peripheral airways. *Am. J. Respir. Crit. Care. Med.* 159:1101–1107.

Frigeri, A., M. Gropper, C.W. Turck, and A.S. Verkman. 1995. Immunolocalization of the mercurial-insensitive water channel and glycerol intrinsic protein in epithelial cell plasma membranes. *Proc. Natl. Acad. Sci. USA.* 92:4328–4331.

Funaki, H., F.H. Yamamoto, Y. Koyama, D. Kondo, E. Yaoita, K. Kawasaki, H, Kobayashi, S. Sawaguchi, H. Abe, and I. Kihara. 1998. Localization and expression of AQP5 in cornea, serous salivary glands, and pulmonary epithelial cells. *Am. J. Physiol.* 275:C1151–C1157.

Hasegawa, H., R. Zhang, A. Dohrman, and A.S. Verkman. 1994. Tissue-specific expression of mRNA encoding the rat kidney water channel CHIP28k by in situ hybridization. *Am. J. Physiol.* 264: C237–C245.

Jayaraman, S., Y. Song, and A.S. Verkman. 2001a. Airway surface liquid osmolality measured using fluorophore-encapsulated liposomes. *J. Gen. Physiol.* 117:423–430.

Jayaraman, S., Y. Song, L. Vetrivel, L. Shankar, and A.S. Verkman. 2001b. Noninvasive in vivo fluorescence measurement of airway surface liquid depth, salt concentration and pH. *J. Clin. Invest.* 107:317–324.

King, L.S., S. Nielsen, and P. Agre. 1997. Aquaporins in complex tissues. I. Developmental patterns in respiratory and glandular tissues of rat. *Am. J. Physiol.* 273:C1541–C1548.

Kreda, S.M., M.C. Gynn, D.A. Fenstermacher, R.C. Boucher, and S.E. Gabriel. 2001. Expression and localization of epithelial aquaporins in the adult human lung. *Am. J. Respir. Cell Mol. Biol.* 24: 224–234.

Ma, T., and A.S. Verkman. 1999. Aquaporin water channels in gastrointestinal physiology. *J. Physiol.* 517:317–326.

Ma, T., B. Yang, A. Gillespie, E.J. Carlson, C.J. Epstein, and A.S. Verkman. 1997. Generation and phenotype of a transgenic knock-out mouse lacking the mercurial-insensitive water channel aquaporin-4. *J. Clin. Invest.* 100:957–962.

Ma, T., B. Yang, A. Gillespie, E.J. Carlson, C.J. Epstein, and A.S. Verkman. 1998. Severely impaired urinary concentrating ability in transgenic mice lacking aquaporin-1 water channels. *J. Biol. Chem.* 273:4296–4299.

Ma, T., Y. Song, A. Gillespie, E.J. Carlson, C.J. Epstein, and A.S. Verkman. 1999. Defective secretion of saliva in transgenic mice lacking aquaporin-5 water channels. *J. Biol. Chem.* 274:20071–20074.

Ma, T., N. Fukuda, Y. Song, M.A. Matthay, and A.S. Verkman. 2000a. Lung fluid transport in aquaporin-5 knockout mice. *J. Clin. Invest.* 105:93–100.

Ma, T., Y. Song, B. Yang, A. Gillespie, E.J. Carlson, C.J. Epstein, and A.S. Verkman. 2000b. Nephrogenic diabetes insipidus in mice lacking aquaporin-3 water channels. *Proc. Natl. Acad. Sci. USA.* 97: 4386–4391.

Manley, G.T., M. Fujimura, T. Ma, F. Filiz, A. Bollen, P. Chan, and A.S. Verkman. 2000. Aquaporin-4 deletion in mice reduces brain edema following acute water intoxication and ischemic stroke. *Nat. Med.* 6:159–163.

Matsui, H., C.W. Davis, R. Tarran, and R.C. Boucher. 2000. Osmotic water permeability of cultured, well-differentiated normal and cystic fibrosis airway epithelia. *J. Clin. Invest.* 105:1419–1427.

Matthay, M.A., H. Folkesson, and A.S. Verkman. 1996. Salt and water transport across alveolar and distal airway epithelia in the adult lung. *Am. J. Physiol.* 270:L487–503.

McFadden, E.R. 1992. Heat and water exchange in human airways. *Am. Rev. Respir. Dis.* 146:S8–S10.

McRae, R.D., A.S. Jones, P. Young, and J. Hamilton. 1995. Resistance, humidity and temperature of the tracheal airway. *Clin. Otolaryngol.* 20:355–356.

Nakhoul, N.L., B.A. Davis, M.F. Romero, and W.F. Boron. 1998. Effects of expressing the water channel aquaporin-1 on the CO_2 permeability of *Xenopus* oocytes. *Am. J. Physiol.* 274:C543–C548.

Nielsen, S., B.L. Smith, E.I. Christensen, and P. Agre. 1993. Distribution of the aquaporin CHIP in secretory and resorptive epithelia and capillary endothelia. *Proc. Natl. Acad. Sci. USA.* 90:7275–7279.

Nielsen, S., L.S. King, B.M. Christensen, and P. Agre. 1997. Aquaporins in complex tissues. II. Subcellular distribution in respiratory and glandular tissues of rat. *Am. J. Physiol.* 273:C1549–C1561.

Noone, P.G., K.N. Oliver, and M.R. Knowles. 1994. Modulation of the ionic milieu of the airway in health and disease. *Annu. Rev. Med.* 45:421–434.

Pilewski, J.M., and R.A. Frizzell. 1999. Role of CFTR in airway disease. *Physiol. Rev.* 79:S215–S255.

Quinton, P.M. 1994. Viscosity vs. composition in airway pathology. *Am. J. Respir. Crit. Care Med.* 149:6–7.

Schnermann, J., J. Chou, T. Ma, M.A. Knepper, and A.S. Verkman. 1998. Defective proximal tubule reabsorption in transgenic aqua-

porin-1 null mice. *Proc. Natl. Acad. Sci. USA*. 95:9660–9664.

Song, Y., N. Fukuda, C. Bai, T. Ma, M.A. Matthay, and A.S. Verkman, A.S. 2000a. Role of aquaporins in alveolar fluid clearance in neonatal and adult lung, and in oedema formation following acute lung injury: studies in transgenic aquaporin null mice. *J. Physiol.* 525:771–779.

Song, Y., T. Ma, M.A. Matthay, and A.S. Verkman. 2000b. Role of aquaporin-4 in airspace-to-capillary water permeability in intact mouse lung measured by a novel gravimetric method. *J. Gen. Physiol.* 115:17–27.

Song, Y., B. Yang, M.A. Matthay, T. Ma, and A.S. Verkman. 2000c. Role of aquaporin water channels in pleural fluid dynamics. *Am. J. Physiol.* 279:C1744–C1750.

Tabka, Z., A. Ben Jebria, J. Vergeret, and H. Guenard. 1988. Effect of dry warm air on respiratory water loss in children with exercise-induced asthma. *Chest.* 94:81–86.

Tsu, M.E., A.L. Babb, E.M. Sugiyama, and M.P. Hlastala. 1991. Dynamics of soluble gas exchange in the airways: II. Effects of breathing conditions. *Respir. Physiol.* 83:261–276.

Verkman, A.S., M.A. Matthay, and Y. Song. 2000a. Aquaporin water channels and lung physiology. *Am. J. Physiol.* 278:L867–L879.

Verkman, A.S., B. Yang, Y. Song, G.T. Manley, and T. Ma. 2000b. Role of water channels in fluid transport studied by phenotype analysis of aquaporin knockout mice. *Exp. Physiol.* 85:233s–241s.

Williams, R., N. Rankin, T. Smith, D. Galler, and P. Seakins, P. 1996. Relationship between the humidity and temperature of inspired gas and the function of the airway mucosa. *Crit. Care Med.* 24: 1920–1929.

Willumssen, N.J., C.W. Davis, and R.C. Boucher. 1994. Selective response of human airway epithelia to luminal but not serosal solution hypertonicity. Possible role for proximal airway epithelia as an osmolality transducer. *J. Clin. Invest.* 94:779–787.

Wine, J.J. 1999. The genesis of cystic fibrosis lung disease. *J. Clin. Invest.* 103: 309–312.

Yager, D., R.D. Kamm, and J.M. Drazen. 1995. Airway wall liquid. Source and role as an amplifier of bronchoconstriction. *Chest.* 107:105S–110S.

Yang, B., N. Fukuda, A.N. van Hoek, M.A. Matthay, T. Ma, and A.S. Verkman. 2000. Carbon dioxide permeability of aquaporin-1 measured in erythrocytes and lung of aquaporin-1 null mice and in reconstituted proteoliposomes. *J. Biol. Chem.* 275:2686–2692.

Yang, B., A. Gillespie, E.J. Carlson, C.J. Epstein, and A.S. Verkman. 2001a. Neonatal mortality in an aquaporin-2 knockout mouse model of recessive nephrogenic diabetes insipidus. *J. Biol. Chem.* 276:2775–2779.

Yang, B., T. Ma, and A.S. Verkman. 2001b. Erythrocyte water permeability and renal function in double knockout mice lacking aquaporin-1 and aquaporin-3. *J. Biol. Chem.* 276:624–628.